Received: 30 May 2017 | Revised: 28 September 2017 | Accepted: 27 February 2018

DOI: 10.1002/eco.1969

RESEARCH ARTICLE

WILEY

Integrated analysis of flow, form, and function for river management and design testing

Belize A. Lane[1] | Gregory B. Pasternack[2] | Samuel Sandoval-Solis[2]

[1] Department of Civil and Environmental Engineering, Utah State University, 4110 Old Main Hill, Logan, UT 84321-4110, USA

[2] Department of Land, Air and Water Resources, University of California Davis, One Shields Ave, Davis, CA 95616, USA

Correspondence
Belize A. Lane, Department of Civil and Environmental Engineering, Utah State University, 4110 Old Main Hill, Logan, UT 84321, USA.
Email: belize.lane@usu.edu

Funding information
USDA National Institute of Food and Agriculture, Grant/Award Numbers: CA-D-LAW-2243-H and #CA-D-LAW-7034-H; UC Davis Hydrologic Sciences Graduate Group

Abstract

The extent and timing of many river ecosystem functions is controlled by the interplay of streamflow dynamics with the river corridor shape and structure. However, most river management studies evaluate the role of either flow or form without regard to their dynamic interactions. This study develops an integrated modelling approach to assess changes in ecosystem functions resulting from different river flow and form configurations. Moreover, it investigates the role of temporal variability in such flow–form–function trade-offs. The use of synthetic, archetypal channel forms in lieu of high-resolution topographic data reduces time and financial requirements, overcomes site-specific topographic features, and allows for evaluation of any morphological structure of interest. In an application to California's Mediterranean-montane streams, the interacting roles of channel form, water year type, and hydrologic impairment were evaluated across a suite of ecosystem functions related to hydrogeomorphic processes and aquatic habitat. Channel form acted as the dominant control on hydrogeomorphic processes, whereas water year type controlled salmonid habitat functions. Streamflow alteration for hydropower increased redd dewatering risk and altered aquatic habitat availability. Study results highlight critical trade-offs in ecosystem function performance and emphasize the significance of spatio-temporal diversity of flow and form at multiple scales for maintaining river ecosystem integrity. The proposed approach is broadly applicable and extensible to other systems and ecosystem functions, where findings can be used to inform river management and design testing.

KEYWORDS

channel classification, ecohydraulics, hydrogeomorphic, Mediterranean montane, river ecosystem function

1 | INTRODUCTION

Rivers are complex, dynamic systems that support many natural ecosystem functions, including hydrogeomorphic processes and the creation and maintenance of aquatic and riparian habitat (Doyle, Stanley, Strayer, Jacobson, & Schmidt, 2005). The extent and timing of these functions is largely controlled by the interplay of *flow*, described by streamflow magnitude, timing, duration, frequency, and rate-of-change (Poff et al., 1997), and *form*, described by the shape and composition of the river corridor (Pasternack, Bounrisavong, & Parikh, 2008; Small, Doyle, Fuller, & Manners, 2008; Vanzo, Zolezzi, & Siviglia, 2016; Wohl et al., 2015; Worthington, Brewer, Farless, Grabowski, & Gregory, 2014). In spite of this complex interplay, most environmental river management studies evaluate the role of either flow or form without regard for these interactions.

The few studies that have effectively examined flow–form interactions related to ecosystem functions highlight the scientific and management value of such analyses. For instance, by evaluating the potential for shallow water habitat in both the historic and current lower Missouri River under alternative flow regimes, Jacobson and

Galat (2006) informed restoration priorities for the river. However, this and similar studies (Brown & Pasternack, 2008; Gostner, Parasiewicz, & Schleiss, 2013; Price, Humphries, Gawne, Thoms, & Richardson, 2013) are site specific, limiting their applicability to the range of flow and form settings exhibited by a given hydroscape, each combination supporting distinct ecosystem functions. Vanzo et al. (2016) offer an exception in their evaluation of ecohydraulic responses to hydropeaking over a spectrum of existing and proposed flows and forms. See Section S1 for more details on the flow–form–function conceptual framework.

Utilizing archetypal channel forms in lieu of detailed, site-specific datasets allows for the evaluation of a larger range of flow–form settings with limited data and financial requirements. An archetype refers to a simple example exhibiting typical qualities of a particular group without the full local variability distinguishing members of the same group (Cullum, Brierley, Perry, & Witkowski, 2017). An archetype-based analysis of the Yuba River, California, was employed by Escobar-Arias and Pasternack (2011), who evaluated salmonid habitat conditions across archetypal 1D cross sections. An emerging technique for synthesizing digital terrain models (DTMs) of river corridors using mathematical functions (Brown, Pasternack, & Wallender, 2014) provides an opportunity to expand on the work of Escobar-Arias and Pasternack (2011) to evaluate 2D hydraulic response across any channel or floodplain morphology of interest without a major increase in data requirements.

The application of synthetic DTMs to the evaluation of river ecosystem performance bypasses data constraints of previous studies through the ability to directly generate representations of historic, existing, or proposed morphologies with user-defined geomorphic attributes. Synthetic river corridors have been used to evaluate controls on pool–riffle salmonid habitat quality and erosion potential as well as to test the occurrence of the hydrogeomorphic mechanism of flow convergence routing across a range of archetypal morphologies (Brown, Pasternack, & Lin, 2015) but have not yet been applied to the development of ecohydraulic design criteria. At the rapid rate of river habitat change and biodiversity loss (Magilligan & Nislow, 2005), the ability to design and compare the ecohydraulic performance of distinct morphologies with relevance beyond an individual study site to an entire watershed or region would offer a powerful tool to support the design of functional large-scale river rehabilitation measures.

1.1 | Study objectives

This study applied synthetic DTMs of archetypal river morphologies, developed at the regional scale based on an existing channel classification, to the evaluation of regional flow–form–function linkages. The authors investigate the common notions of flow- and form-process linkages, in which different flow regimes and morphologies are assumed to support distinct hydrogeomorphic processes (Kasprak et al., 2016; Montgomery & Buffington, 1997; Poff et al., 1997). The overall goal of the study is to test whether archetypal combinations of flow and form attributes generate quantifiable hydraulic patterns that support distinct ecosystem functions. The study objectives are to (1) generate synthetic DTMs of distinct river corridor archetypes mindful of patterns of topographic variability necessary to ecogeomorphic dynamics, (2) evaluate the spatio-temporal patterns of depth and velocity across the archetypal DTMs from Objective 1, and (3) quantify the performance of a suite of critical ecosystem functions across alternative flow–form scenarios. The specific scientific questions addressed through these objectives are as follows: (a) Do archetypal river corridor morphologies support distinct ecosystem functions or is more or different local topographic variation within archetypes needed? (b) What is the significance of subreach-scale topographic variability in river ecosystem functioning? (3) What is the role of water year type and hydrologic impairment? (d) What ecosystem performance trade-offs can be identified with relevance for environmental water management?

1.2 | Case study setting: Mediterranean-montane rivers

Mediterranean-montane river systems, which exhibit cold wet winters and warm dry summers, provide a useful setting for evaluating flow–form interactions because they exhibit significant variability to test system sensitivity to different drivers (Gasith & Resh, 1999). In the California Sierra Nevada, USA, native aquatic and riparian species are adapted to the biotic stresses (e.g., reduced water quality in summer) and abiotic stresses (e.g., high shear stress during winter floods) associated with the highly seasonal flow regimes that depend on flow–form interactions. Salmonid eggs, for example, require sufficient inundation depths and intragravel flows in certain channel locations during biologically significant periods to survive (U.S. Fish and Wildlife Service [USFWS], 2010a). Sierra Nevada rivers have been highly altered by dams and reservoir operations for water supply, flood control, and hydropower (Hanak et al., 2011), driving dramatic declines in native aquatic populations (Moyle & Randall, 1998; Yarnell, Lind, & Mount, 2012; Yoshiyama, Fisher, & Moyle, 1998). See Section S1.2 for more details.

2 | METHODS

The methodology can be summarized by three steps (Figure 1). First, a set of synthetic river corridor DTMs is generated to represent channel types from an existing channel classification (Section 2.1), and a set of hydrologic scenarios is selected for evaluation (Section 2.2). Next, a 2D hydrodynamic model (sedimentation and river hydraulics-two dimensional [SRH-2D]; Lai, 2008) is used to simulate ecologically relevant hydraulic parameters (ERHPs, sensu Vanzo et al., 2016) for each flow–form scenario (Sections 2.3 and 2.4). Finally, spatio-temporal patterns in ERHPs are used to evaluate the performance or occurrence of a suite of ecosystem functions (Section 2.5) under each scenario. Each of these steps is described in depth in the following paragraphs.

Specifically, selected streamflow time series (flows) and river corridor DTMs (forms) are input to a 2D hydrodynamic model to produce a continuum of hydraulic rasters (i.e., depth [d], velocity [v], and shear stress [τ]) for a modelled river corridor at each modelled flow stage. For each model run, a set of ERHP rasters (e.g., Shields stress [τ_o^*], indices incorporating both depth and velocity [$d{\cdot}v$]) is calculated from hydraulic model raster outputs. Finally, spatial and temporal statistics

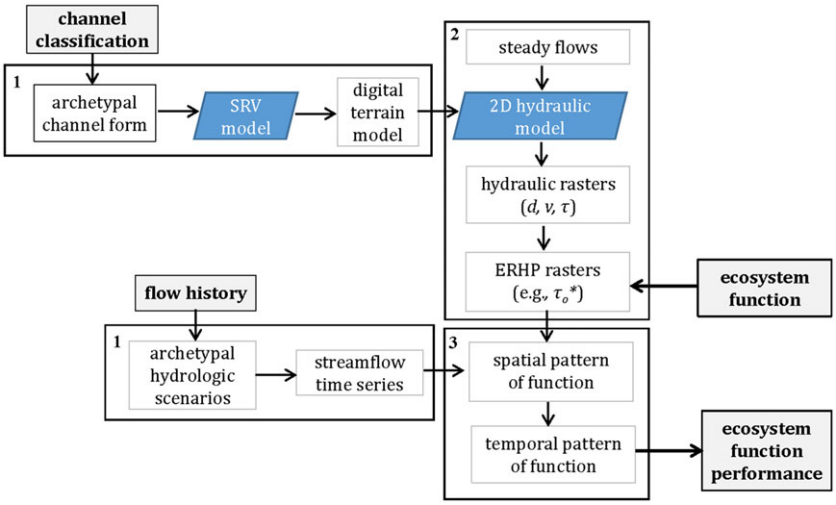

FIGURE 1 Major steps used to quantify ecosystem function performance across archetypal channel forms and hydrologic scenarios, with step numbers associated with text above. Key inputs and outputs are bolded, and modelling tools are blue parallelograms

characterizing ERHP outputs are used first to evaluate model results in terms of depth and velocity at baseflow (0.2× bankfull), 50% exceedance, and bankfull flows, and then to quantify the performance of distinct ecosystem functions. Bankfull discharge, defined as the flow that just reaches the transition between the channel and its floodplain, was estimated from the channel geometry as described in Section 2.4. Temporal dynamics are evaluated by integrating ERHP spatial statistics over each hydrologic scenario (Parasiewicz, 2007) such that not only the magnitude but also the timing, duration, and frequency of ecosystem functions can be evaluated depending on the particular temporal requirements. The resulting annual time series represent the temporal pattern of the 2D hydraulic response in a specific DTM for a single hydrologic scenario. This process is detailed in Section S2.

The experimental design involved a series of 16 hydraulic model runs under steady flow conditions, simulating two river corridor morphologies across eight discharges spanning baseflow (0.2× bankfull) to twice bankfull flow stages. The decision to evaluate proportions of bankfull flow was driven by the established geomorphic and ecological significance of bankfull flow in the literature (Doyle et al., 2005; Richter & Richter, 2000; Wolman & Miller, 1960). Further, scaling flows by a common nondimensional metric allows for readers worldwide to evaluate these results relative to the setting in their locality. These eight discharges discretized the daily flow regimes evaluated to simplify temporal analysis. All simulated combinations were designed to reproduce realistic archetypal flow and form conditions in Mediterranean-montane river systems for two channel types of interest, plane bed and pool–riffle (see Section 2.1). A rigorous scaling approach to compare the full range of possible configurations was outside the scope of the current study. The following sections describe the flow regimes, river corridor morphologies, hydraulic modelling approach, and ecosystem functions considered.

2.1 | Synthetic river corridor morphologies

Two archetypal river corridor morphologies distinguished in the Sacramento Basin channel classification by Lane, Pasternack, Dahlke, and Sandoval-Solis (2017) were considered in this study as a proof of concept: semiconfined plane bed and semiconfined pool–riffle. These morphologies were selected for their common occurrence in midelevation montane environments (Montgomery & Buffington, 1997; Wohl & Merritt, 2005) and their similar channel dimensions and slopes contrasted by major differences in subreach-scale topographic variability. An existing field data-driven channel classification for the Sacramento Basin (Lane, Pasternack, et al., 2017) provided the parameter values needed to synthesize the two archetypal morphologies, quantified as the median field-surveyed values for each channel type.

DTMs of the investigated channel types were generated using the synthetic rivers model developed by Brown et al. (2014). Below, we briefly provide the equations vital to understanding the DTMs created in this study. The goal of the design process was to capture the essential organized features of each channel type so that their functionalities can be evaluated in a reductionist approach without the random details of real river corridors that cause highly localized effects.

2.1.1 | Reach-average parameters

The synthetic rivers approach first creates a reach-averaged river corridor that is scaled by reach-averaged bankfull width (w_{BF}) and bankfull depth (h_{BF}), with median sediment size (D_{50}), slope (S), sinuosity, and floodplain width and lateral slope as user-defined input variables. For each synthetic river scenario, 140 longitudinal nodes were spaced at 1 m (~1/10 bankfull channel widths).

2.1.2 | Channel variability functions

Next, this approach incorporates subreach-scale (<10 channel widths frequency) topographic variability because many hydrogeomorphic processes of ecological significance depend on specific patterns of topographic variability and associated habitat heterogeneity (MacWilliams, Wheaton, Pasternack, Street, & Kitanidis, 2006; Poff & Ward, 1990; Scown, Thoms, & De Jager, 2015). The local bankfull width at each location x_i along the channel, $w_{BF}(x_i)$, is given by Equation 1 as a function of reach-averaged bankfull width w_{BF} and a variability control function $f(x_i)$, with a similar equation used to characterize vertical bed undulation that incorporates S:

$$w_{BF}(x_i) = w_{BF}{}^{*} f(x_i) + w_{BF}. \quad (1)$$

There are many available mathematical and statistical control functions that may be used to describe archetypal river variability (Brown & Pasternack, 2016). For this study, the variability of w_{BF} and h_{BF} about the reach-averaged values was determined by a sinusoidal function, as

$$f(x_i) = a_s \sin(b_s x_r + h_s), \quad (2)$$

where a_s, b_s, and h_s are the amplitude, angular frequency, and phase shift alignment parameters for the sinusoidal component, respectively, and x_r is the Cartesian stationing in radians. The Cartesian stationing was scaled by w_{BF} so that the actual distance was given by $x_i = x_r{}^{*} w_{BF}$. The sinusoidal function alignment parameters were adjusted iteratively to achieve desired values for h_{BF}, width-to-depth ratio (w/h_{BF}), sinuosity, and the coefficient of variation (CV) of w_{BF} and h_{BF} based on plane bed and pool–riffle channel classification archetypes (Lane, Pasternack, et al., 2017). Floodplain confinement, the bankfull to floodplain width ratio, was used to set valley width and overbank topography.

Because river classifications traditionally aim to capture the central tendency of river types at the reach scale, they contain little to no information on subreach-scale topographic variability and landform patterning (Lane, Pasternack, et al., 2017). This study used outputs from a channel classification that was unique in including statistical characterization of subreach width and depth variability using the metric of CV based on the average and standard deviation of field-derived values (Lane, Pasternack, et al., 2017). However, there remained numerous landform patterning permutations using the control function parameters of Equation 2 that could yield those CV values, many associated with profoundly different geomorphic processes. In these cases, field experience and judgment informed the design of topographies capable of supporting the dominant geomorphic processes of each channel type as outlined in the classification study. For example, for the pool–riffle system, minimum depth and maximum width were made to positively covary in the DTM to represent this patterning (Brown & Pasternack, 2016).

2.2 | Flow regimes

Four hydrologic scenarios characteristic of the mixed snowmelt and rain flow regime typical of Mediterranean-montane systems were evaluated (Lane, Dahlke, Pasternack, & Sandoval-Solis, 2017): unimpaired wet, unimpaired dry, altered wet, and altered dry annual flow regimes (Figure 2). Daily streamflow time series for two midelevation gauge stations in the western Sierra Nevada, California, were chosen to represent these archetypal flow regimes under unimpaired (North Yuba River below Goodyears Bar) and altered (New Colgate Powerhouse) conditions (see Section S2.2 for map of gauge locations). These gauges lie within similar physioclimatic and geologic settings and provide daily streamflow time series for both an extremely wet (WY 2010; >75th percentile annual streamflow) and an extremely dry (WY 2014; <25th percentile annual streamflow) water year. The New Colgate Powerhouse gauge captures typical hydropeaking patterns of Sierra Nevada streams. The 50% exceedance flows for each hydrologic scenario are 23.3, 5.0, 19.2, and 18.5 m^3/s for the wet unimpaired, dry unimpaired, wet altered, and dry altered scenarios, respectively.

2.3 | Hydraulic modelling

The surface-water modelling system (Aquaveo, LLC, Provo, UT) user interface and SRH-2D algorithm (Lai, 2008) were used to produce exploratory hydrodynamic models for each flow–form scenario. SRH-2D is a finite-volume numerical model that solves the Saint Venant equations for the spatial distribution of water surface elevation, water depth, velocity, and bed shear stress at each computational node. It

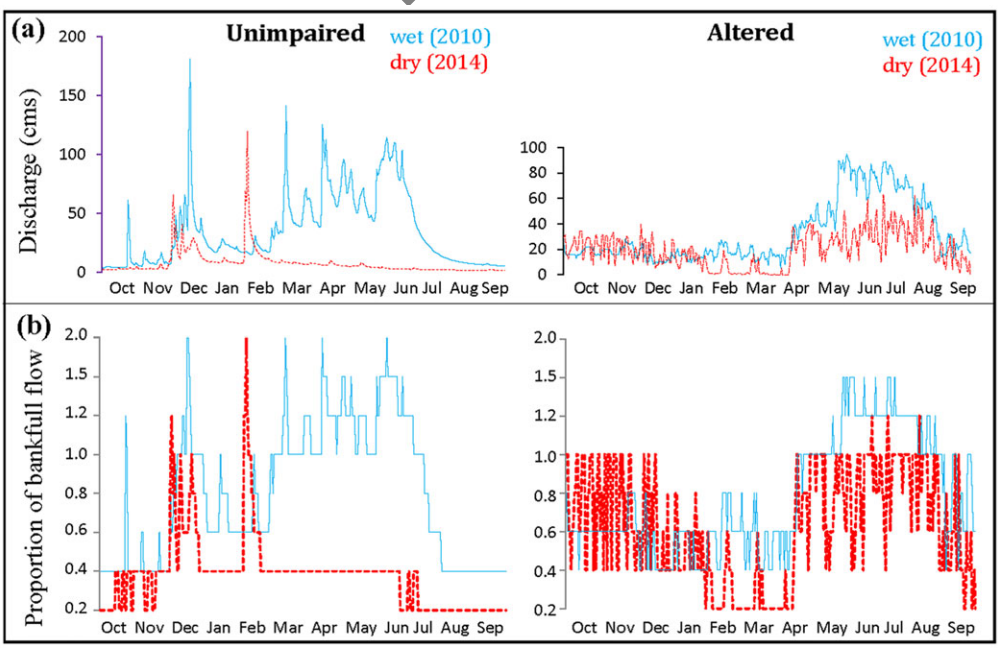

FIGURE 2 Four hydrologic scenarios were considered: unimpaired wet, unimpaired dry, altered wet, and altered dry. Graphs illustrate unimpaired and altered daily time series of (a) streamflow and (b) discretized proportions of bankfull flow based on stage–discharge thresholds from Table 1

can handle wetting/drying and supercritical flows among other features. The parametric eddy viscosity equation was used for turbulence closure. A coefficient value of 0.1 suitable for shallow rivers with coarse bed sediment was used in that equation. A computational mesh with internodal mesh spacing of 1 m (relative to a channel width of 10 m) was generated for each synthetic DTM. Because this study was purely exploratory, using numerical models of theoretical river archetypes, no calibration of bed roughness or eddy viscosity was possible. Similarly, no validation of model results was possible.

The model required inputs of discharge and downstream flow stage as well as boundary conditions of bed topography and roughness. Eight model runs for each morphology capture the discharge range of 0.2–2.0× bankfull flow stage (Table 1), where bankfull flow stage is the water surface elevation at which flows spill onto the floodplain. The specific simulated discharge values associated with these stages were estimated for each morphology using Manning's equation based on representative cross sections of the synthetic DTMs. Bankfull stage and wetted perimeter were determined manually from the cross sections, and cross-sectional area was calculated using the trapezoidal approximation. Manning's n was set at 0.04 to represent a typical unvegetated gravel/cobble surface roughness (Abu-Aly et al., 2014).

2.4 | Hydrological scaling

Finally, in order to scale the real streamflow time series to the synthetic DTMs, stage–discharge relationships are needed to associate each of the eight flow stages simulated in the hydraulic model (Table 1) with the actual discharge required to fill the North Fork Yuba river channel to that flow stage. In the absence of local stage–discharge relationships, these thresholds were instead estimated manually (Table 1, final column) with the aim of retaining archetypal hydrologic characteristics of interest. Specifically, stage thresholds were set so, in the wet year, the flow stage time series remained at or above bankfull during winter storms and throughout the spring snowmelt recession, whereas, in the dry year, flow stage rarely exceeded bankfull and spent the majority of summer at base flow. The estimated stage–discharge thresholds were justified by the ability of the discretized flow regimes (Figure 2b) to retain these hydrologic patterns exhibited by the undiscretized flow regimes (Figure 2a). However, these thresholds are estimates and should not be considered as ultimate targets to inform river management. A major assumption of this approach is that the flow stage discretization captures all significant spatial hydraulic patterns in the river corridor relative to the functions under consideration in this study (see Supporting Information for more details).

2.5 | River ecosystem functions

Five Mediterranean-montane ecosystem functions were considered, associated with two major components of river ecosystem integrity: hydrogeomorphic processes and aquatic habitat (Table 2). The performance of these functions was tested based on the following criteria: (1) a longitudinal shift in the location of peak shear stress at high flows from topographic highs to topographic lows was used to test the occurrence of flow convergence routing, a dominant geomorphic formation and maintenance process in certain channels (MacWilliams et al., 2006); (2) a measure of hydrogeomorphic variability was used to quantify overall habitat heterogeneity in the river corridor (Gostner, Alp, et al., 2013); and (3) fall-run Chinook salmon habitat was evaluated with respect to (a) bed preparation and (b) bed occupation functions based on established shear stress thresholds and biologically significant timing thresholds (Escobar-Arias & Pasternack, 2010) as well as (c) redd dewatering risk during bed occupation. These functions were evaluated using a Python script that enabled rapid evaluation of model outputs over the specific spatio-temporal constraints.

2.5.1 | Flow convergence routing mechanism

Flow convergence routing, the periodic reversal of peak shear stress location, is often considered critical to pool–riffle maintenance (White, Pasternack, & Moir, 2010). The Caamaño criterion (Caamaño, Goodwin, Buffington, Liou, & Daley-Laursen, 2009) was used to estimate the minimum riffle depth needed for a reversal to occur in each archetypal morphology. This mechanism was further evaluated based on the presence of a shift in peak shear stress from topographic wide highs (riffles) to narrow lows (pools), which indicates that the locations of scour and deposition are periodically shifted in the channel to maintain the relief between riffles and pools (Brown & Pasternack, 2014).

2.5.2 | Hydrogeomorphic diversity

The hydromorphological index of diversity (HMID; Gostner, Alp, et al., 2013) was used to quantify overall physical heterogeneity of the river

TABLE 1 Simulated channel archetype discharge values for 0.2–2.0× bankfull flow stage calculated from Manning's equation and associated stage–discharge threshold estimates for the North Yuba River

	Simulated discharge		North Yuba River discharge
Fraction of bankfull flow	Plane bed (m^3/s)	Pool–riffle (m^3/s)	Stage–discharge threshold (m^3/s)
0.2	1.3	1.2	2.8
0.4	6.8	4.5	14.2
0.6	17.7	9.7	22.7
0.8	28.7	17.8	28.3
1.0	58.2	27.7	56.6
1.2	95.5	64.3	85.0
1.5	164.4	139.9	113.3
2.0	310.3	338.1	141.6

TABLE 2 The five river ecosystem functions evaluated in this study and their associated ecologically relevant hydraulic parameters (ERHPs), biologically relevant periods, and spatial extents

Ecosystem function	ERHP(s)	Biological period	Spatial extent	Citation
Hydrogeomorphic processes				
Flow convergence routing	Shear stress	—	Bankfull channel	MacWilliams et al. (2006)
Hydrogeomorphic diversity	Velocity, depth	—	River corridor	Gostner, Alp, Schleiss, and Robinson (2013)
Aquatic habitat				
Salmonid bed preparation	Shear stress	October–March	Bankfull channel	Escobar-Arias and Pasternack (2010)
Salmonid bed occupation	Shear stress	April–September	Bankfull channel	
Redd dewatering	Velocity, depth	October–March	Spawning channel	USFWS (2010b)

corridor as follows, where the CV is the standard deviation of depth or velocity divided by its mean:

$$HMID_{reach} = (1 + CV_v)^{2*}(1 + CV_d)^2. \quad (3)$$

Three tiers of HMID were delineated as follows: HMID <5 indicates simple uniform or channelized reaches; 5 < HMID < 9 indicates a transitional range from uniform to variable reaches; and HMID > 9 indicates morphologically complex reaches (Gostner, Parasiewicz, et al., 2013). To date, no studies have applied this index to archetypal terrains, so this is a novel application to further understand its value in quantifying ecosystem functions. Percent exceedance curves of HMID provided graphical representations of the temporal patterns of hydraulic diversity under alternative flow–form scenarios.

2.5.3 | Salmonid bed occupation and preparation

Ecosystem functions related to salmonid habitat can be split into (a) bed occupation functions, which occur while the fish are directly interacting with the channel bed (i.e., spawning, incubation, and emergence), and (b) bed preparation functions, which occur between occupation periods during migration (Escobar-Arias & Pasternack, 2011). A stable bed, indicated by low shear stress ($\tau_o^* < \tau_{c\,50}$), is needed to minimize scour during bed occupation (October–March), whereas high shear stress capable of mobilizing the active layer ($\tau_o^* > \tau_{c\,50}$) is necessary to rejuvenate the sediment during bed preparation (April–September) (Konrad, Booth, Burges, & Montgomery, 2002; Soulsby, Youngson, Moir, & Malcolm, 2001). See Section S2.5.4 for more details.

Bed mobility transport stages delimited per pixel by nondimensional boundary shear stress or Shields stress (τ_o^*) thresholds (Jackson, Pasternack, & Wheaton, 2015) were used to quantify these bed occupation and preparation functions according to the following equation:

$$\tau_o^* = \frac{\tau_b}{g(\rho_s - \rho)D_{50}}, \quad (4)$$

where $\tau_b$is bed shear stress

$$\tau_b = \rho_w \left(u^*\right)^2, \quad (5)$$

based on water density (ρ_w) and shear velocity $u^* = U\sqrt{C_d}$, where U is depth-averaged velocity for an individual pixel, and C_d is the depth-based drag coefficient (Pasternack, 2011). τ_o^* therefore varies spatially and with discharge as a function of depth and velocity. For the present application, a stable bed is assumed when $\tau_o^* < 0.01$, intermittent transport when $0.01 < \tau_o^* < 0.03$, partial transport when $0.03 < \tau_o < 0.06$, and full mobility when $0.06 < \tau_o^* < 0.10$ (Buffington & Montgomery, 1997). At each discharge, the areal proportion of each bed mobility tier occurring in the river corridor region of interest can be calculated. Function performance is then quantified through time as the cumulative proportion of the channel providing functional bed mobility conditions during biologically relevant periods. Results are then binned such that low, mid, and high performances are associated with 0–25%, 25–75%, and 75–100% performance. For example, at least 75% of the channel area must exhibit partial or full bed mobility on average over the bed preparation period to achieve high bed preparation performance.

2.5.4 | Redd dewatering

Salmonid redd dewatering is a major concern in Sierra Nevada streams managed for hydropower (USFWS, 2010b). Reductions in flow stage exposing the tailspill and reductions in velocity diminishing intragravel flow through the redd can dramatically reduce the survival of salmonid eggs and pre-emergent fry (Healey, 1991; USFWS, 2010b). This study focused on fall-run Chinook salmon (*Oncorhynchus tshawytscha*) as an important species in Sierra Nevada streams. Redd dewatering risk was measured as the areal proportion of viable spawning habitat with depth below 0.15 m and/or velocity below 0.09 m/s during the occupation period (incubation and emergence period [December–March]; USFWS, 2010b). Viable spawning habitat was defined according to USFWS as the portion of the bankfull channel with velocity from 0.1 to 1.6 m/s and depth from 0.15 to 1.3 m at 0.4× bankfull stage, the most common stage experienced under unimpaired conditions during the spawning period (October–December; USFWS, 2010a).

2.6 | Holistic ecosystem functions analysis

There is limited guidance available in the literature regarding how best to evaluate and visually represent the environmental performance of rivers across a suite of ecosystem functions. The question of how best to evaluate environmental performance using individual metrics or functions is well established (CITE). The broader water resources management literature offers several summary performance indices that could be applied to this new setting. For example, the water resources management sustainability index (Sandoval-Solis, McKinney, & Loucks, 2010), which evaluates different water management policies by summarizing across metrics of reliability, resilience, and vulnerability, could

be applied as a summary index of environmental performance. In this study, we created a graphic that aligns all of the ecosystem functions in one table to visualize the performance of a suite of temporally varying functions simultaneously.

3 | RESULTS

The synthetic DTM results are presented first (Study Objective 1). Then the hydraulic modelling results are discussed in terms of depth and velocity patterns (Study Objective 2). Finally, model results are used to interpret the performance of five ecosystem functions (Table 2) across alternative flow–form scenarios (Study Objective 3).

3.1 | Synthetic digital terrain models

Two 140-m-long synthetic DTMs were generated representing archetypal morphological configurations of semiconfined pool–riffle and plane bed morphologies (Figure 3). These DTMs exhibited distinct reach-averaged attributes (e.g., S, w/h_{BF}, and D_{50}; Table 3a), subreach-scale topographic variability (e.g., CV), and proportions of the river corridor exhibiting positive and negative geomorphic covariance structures (GCSs; Table 3b). The sinusoidal function alignment parameters used are listed in Table 3b. The resulting morphologies exhibited major differences in subreach-scale topographic variability as illustrated by the planform and longitudinal topographic patterns in Figure 3. The bankfull channel area was 868 m^2 in the pool–riffle and 1,041 m^2 in the plane bed DTM.

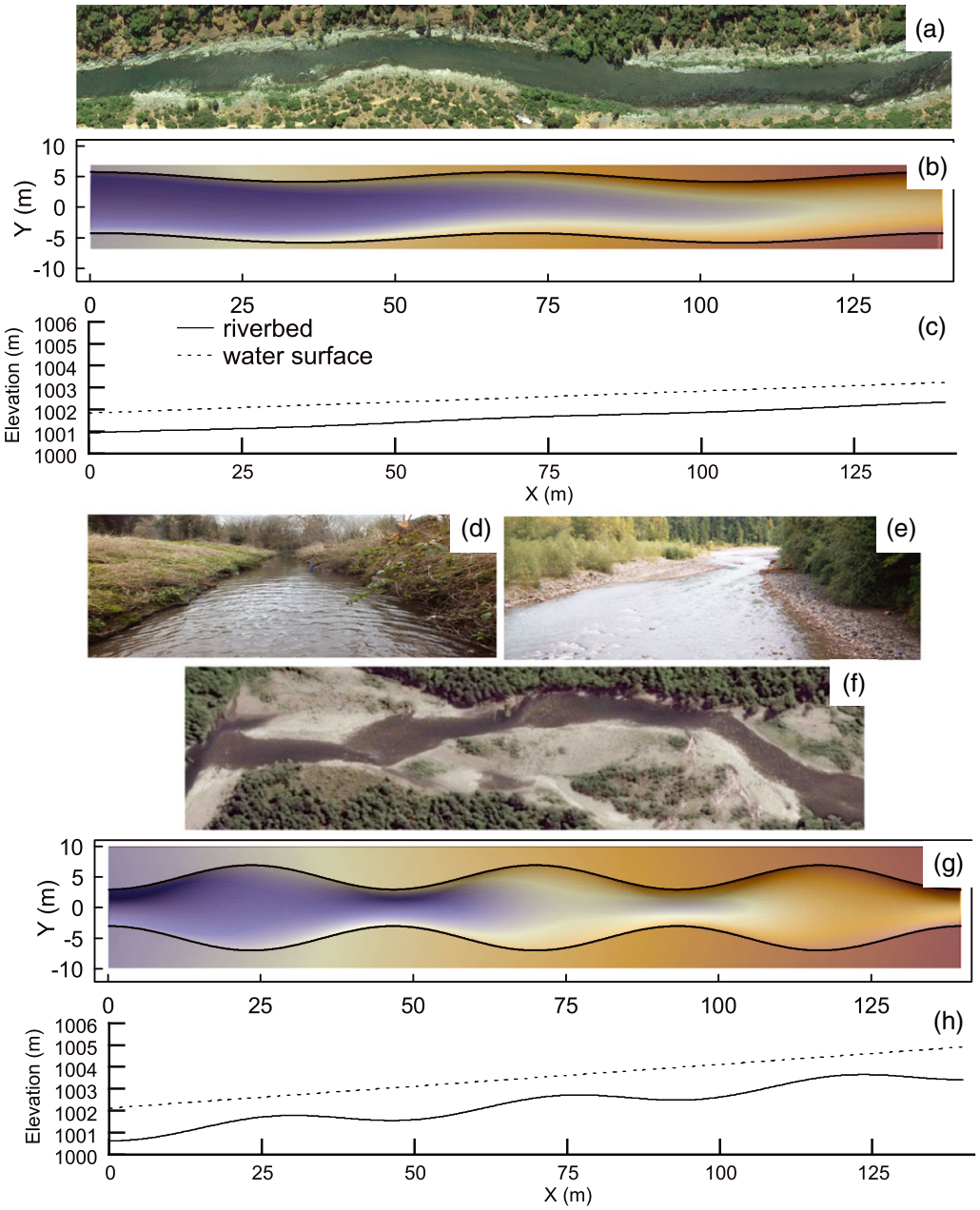

FIGURE 3 Two archetypal river corridor morphologies evaluated in this study, including example images, synthetic DTMs overlaid by bankfull channel boundaries, and longitudinal profiles

TABLE 3 (a) Channel and floodplain geomorphic attributes and (b) control function alignment parameters used in the design of synthetic DTMs of plane bed and pool–riffle channel morphologies

(a) Geomorphic attributes			(b) Alignment parameters		
	Plane bed	Pool–riffle		Plane bed	Pool–riffle
Channel			Planform		
w_{BF} (m)	10	10	Phase shift	0	0
h_{BF} (m)	1	1	Amplitude	0.8	0
S (%)	1	2	Frequency	2	2
w/h_{BF}	10	10	Bankfull Width		
D_{50} (m)	0.2	0.1	Phase shift	π/2	π
Sinuosity	1.1	1.1	Amplitude	0.01	0.5
CVw_{BF}	0.01	0.35	Frequency	2	3
CVH_{BF}	0.03	0.18	Bed elevation		
+GCS (%)	55	86	Phase shift	0	2.7
−GCS (%)	45	14	Amplitude	0.04	0.35
Floodplain			Frequency	2	3
Confinement	0.5	0.5	Floodplain outline		
Lateral slope (%)	0.80	0.80	Phase shift	0	0
Width (m)	16	16	Amplitude	0	0.5
D_{50} (m)	0.03	0.03	Frequency	1.5	1.5

3.2 | Spatial and temporal distribution of hydraulic variables

Depth and velocity values fell within typical ranges for gravel-bed montane streams across base, 50% exceedance, and bankfull flows, supporting the archetypal specifications used in this study (Jowett, 1993; Richards, 1976). Water depths ranged from 0.0 to 2.4 m, with higher average depths in the plane bed than the pool–riffle across all three flows. The pool–riffle had lower minimum and higher maximum depths across all flow levels, resulting in a larger depth range and CV. Flow velocities ranged from 0.0 to 5.5 m/s, exhibiting a similar pattern to depth between morphologies, with higher average and minimum velocities in the plane bed across all eight discharge stages. In contrast with depth, however, at bankfull flow maximum velocity was significantly higher in the plane bed than the pool–riffle, resulting in a higher velocity CV. The HMID was substantially higher at base flow than higher flows and was more than twice as high in the pool–riffle as in the plane bed at base flow.

Time series plots of hydraulic summary statistics illustrate the daily temporal variability of depth and velocity over the four hydrologic scenarios (Figure 4). A reversal in the maximum CV of velocity from the pool–riffle to the plane bed is evident during spring in the wet unimpaired scenario and during summer in the wet altered scenario, corresponding with a very high maximum velocity in the plane bed (5.5 m/s). The remainder of seasons and water year types exhibit higher hydraulic variability in the pool–riffle, with the largest differences in CV occurring at low flows.

Water depth was more sensitive to low flow variations in terms of rate of change, and velocity was more sensitive to changes in high flows. This likely occurs because, in parabolic channel geometries, the channel fills rapidly from low to bankfull flow, whereas, once the bankfull channel is overtopped, a larger flow increase is required to engender the same increase in water depth over the wider floodplain so high flow changes translate more directly to velocity. With regard to channel type, the pool–riffle morphology demonstrated an approximately linear increase in depth with flow, whereas the plane bed morphology demonstrated a rapid increase in depth from low flow to 0.8× bankfull and a reduced rate of increase at higher flows. Conversely, velocity in both morphologies increased at a slow linear rate from low flow to 0.8× bankfull flow and then increased much faster in the plane bed at higher flows. Only at high flows (>1.5× bankfull) did pool–riffle velocity exhibit a strong sensitivity to flow variability. These findings demonstrate that changes in the hydraulic environment due to variations in discharge were stronger in the plane bed than the pool–riffle, indicating that pool–riffle hydraulics are less sensitive to changes in flow on average but instead exhibit more complex spatial patterns.

3.3 | Ecosystem function performance results

All six Mediterranean-montane river ecosystem functions were found to be controlled by both flow and form attributes to varying extents, as illustrated in Figure 5 for the unimpaired flow regime and in Figure 6 for the altered flow regime.

3.3.1 | Flow convergence routing

The pool–riffle morphology demonstrated a shear stress reversal from low to high flow, as indicated by a Caamaño criterion riffle depth threshold for reversal of 0.21 m (approximately 0.4× bankfull stage) and a shift in the location of peak shear stress from the riffle crest to the pool trough from base to bankfull flow (see Supporting Information for more details). The existence of a dominant flow convergence routing mechanism is further indicated by 86% of the pool–riffle morphology exhibiting a positive GCS (i.e., primarily wide shallow riffles and narrow deep pools). Alternatively, the plane bed morphology did not exhibit a shear stress reversal based on either the Caamaño

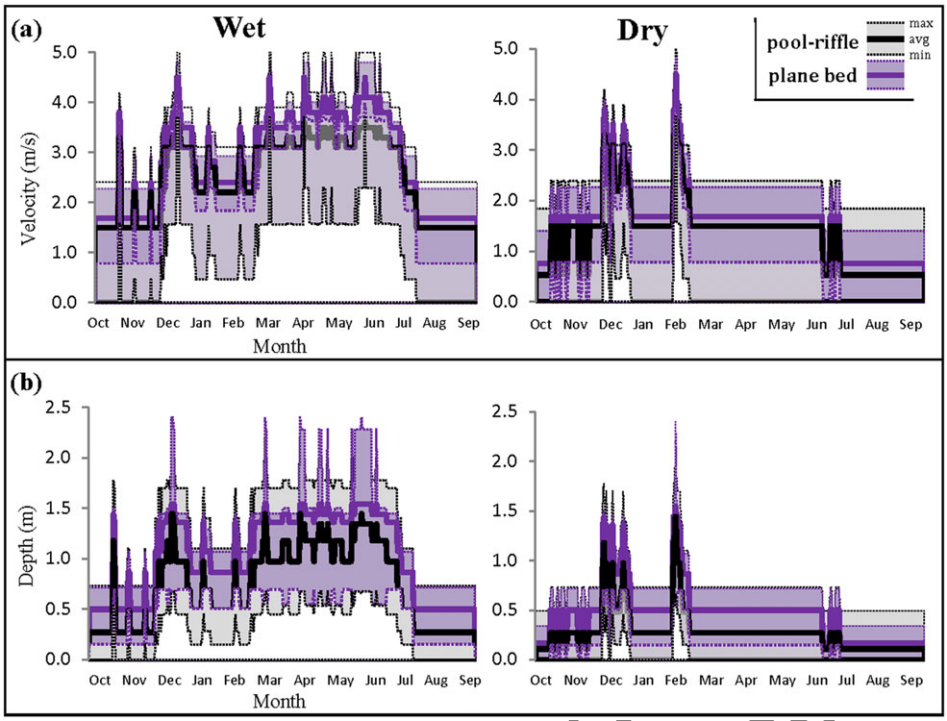

FIGURE 4 Annual time series plots of maximum, average, and minimum (a) flow velocity and (b) water depth in plane bed and pool–riffle morphologies over four hydrologic scenarios

criterion or a peak shear stress location shift, and only 55% of the river corridor exhibited positive GCS.

3.3.2 | Hydrogeomorphic diversity (HMID)

HMID was higher in the pool–riffle than the plane bed morphology at flows up to 1.2× bankfull, beyond which they were nearly equivalent. That is, for a given hydrologic scenario, the cumulative HMID over the year was higher in the pool–riffle. The highest index values and the greatest difference between the two morphologies occurred at the lowest flow stage (0.2× bankfull discharge), when HMID was twice as high in the pool–riffle. The rapid decrease in HMID for in-channel flows in both morphologies with increasing discharge illustrates the limited temporal persistence of high diversity hydraulic habitats in all but the lowest

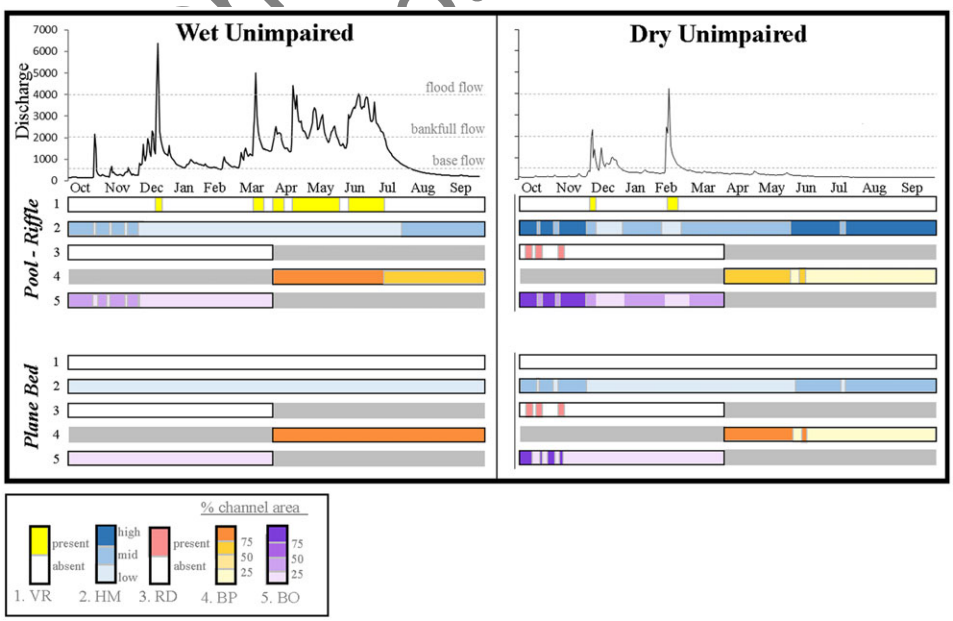

FIGURE 5 Summary of temporally varying ecosystem function performance under an unimpaired flow regime across four flow–form scenarios: wet—pool–riffle, wet—plane bed, dry—pool–riffle, and dry—plane bed. The five ecosystem functions evaluated are (1) flow convergence routing (VR), (2) hydrogeomorphic diversity (HG), (3) redd dewatering risk (RD), (4) salmonid bed preparation (BP), and (5) salmonid bed occupation (BO). Tiered performance is indicated in the key by increasingly dark shading and bimodal performance (VR and RD) is either coloured or empty. Greyed regions indicate periods of the year that functions are not biologically relevant. Base flow = 0.2×, bankfull flow = 1.0×, and flood flow = 1.5× bankfull flow as defined in Table 1

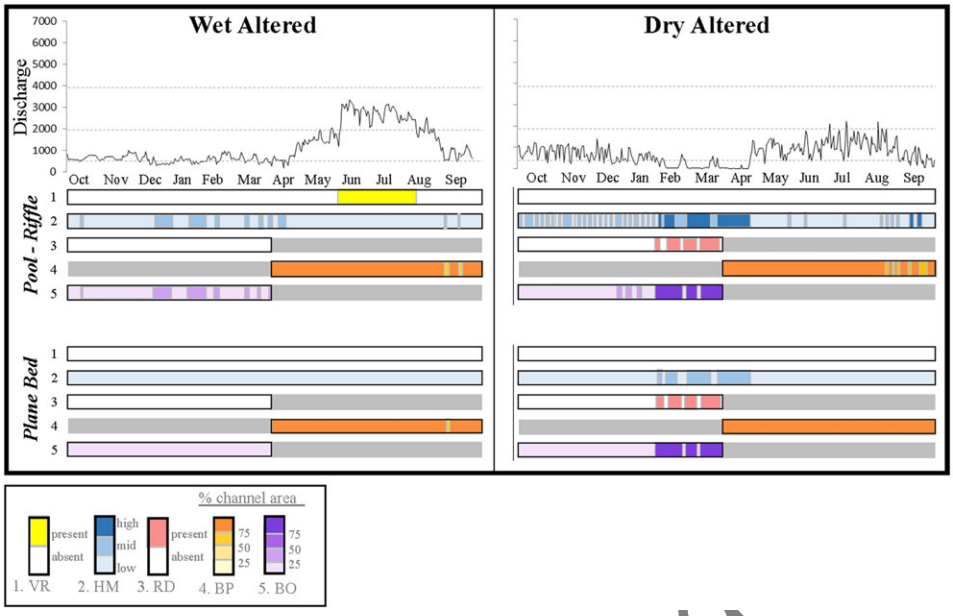

FIGURE 6 Summary of temporally varying ecosystem function performance under an altered flow regime across four flow–form scenarios: wet—pool–riffle, wet—plane bed, dry—pool–riffle, dry—plane bed. The five ecosystem functions evaluated are (1) flow convergence routing (VR), (2) hydrogeomorphic diversity (HG), (3) redd dewatering risk (RD), (4) salmonid bed preparation (BP), and (5) salmonid bed occupation (BO). Tiered performance is indicated in the key by increasingly dark shading and bimodal performance (VR and RD) is either coloured or empty. Greyed regions indicate periods of the year that functions are not biologically relevant

flow conditions. In natural conditions, once flows spill over the banks, there should be a significant increase in HMID as topographically heterogeneous floodplains inundate. However, in the absence of detailed floodplain attributes from the channel classification, this study considered simple floodplain morphologies in both archetypes.

HMID exceedance curves for each of the eight flow–form scenarios provided insight into hydraulic diversity patterns (Figure 7). As low flows produce higher HMID values in general, it is unsurprising that in a very dry year both morphologies exhibited high HMID for most of the year. Under dry conditions, the unimpaired flow regime provided nearly twice as many days with high HMID in both morphologies. Under the altered flow regime, HMID was slightly higher in the wet pool–riffle than the dry plane bed for all flows above 17% exceedance. The highest HMID was exhibited by the pool–riffle under dry unimpaired conditions (HMID = 5.9), presumably due to the combination of high topographic variability and extended summer low flows. At the 50% exceedance flows of each hydrologic scenario, hydraulic diversity was more sensitive to water year type than hydrologic alteration and appeared to be most controlled by channel morphology. Alternatively, at the 10% exceedance flows, water year type played a more significant role, with the dry year exhibiting much higher HMID across both morphologies and impairment conditions. More significantly, the temporal analysis of HMID revealed that, unlike the dry altered flow regime, the dry unimpaired flow regime exhibited high HMID during the fall-run Chinook bed occupation period, as detailed in the Supporting Information.

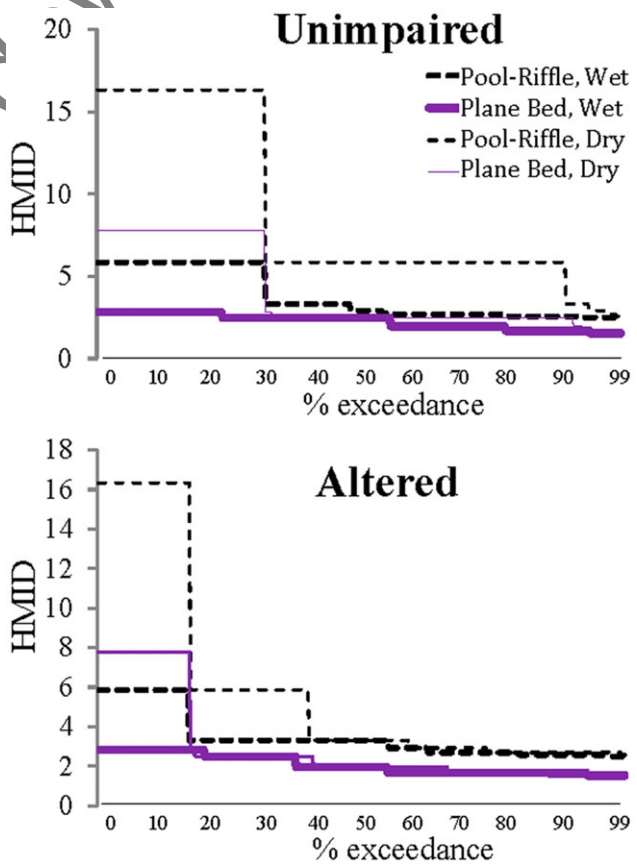

FIGURE 7 Hydromorphic index of diversity (HMID) exceedance curves for (a) unimpaired and (b) altered flow regimes under different channel morphologies and water year types

3.3.3 | Salmonid bed preparation and occupation

Significant differences in salmonid habitat performance across flow–form scenarios were identified from shear stress-based sediment

mobility patterns (Figure 8). Under unimpaired conditions, the wet year exhibited high bed preparation performance and low bed occupation performance, whereas the dry year exhibited midperformance in both functions with reduced bed preparation but increased bed occupation performance. Under streamflow alteration, bed preparation performed well across water years whereas bed occupation performed poorly across water years and morphologies due to increased sediment mobility under elevated low flows during the occupation period. Spatially, in the pool–riffle channel, higher sediment mobility occurred over the riffle crests and the pools remained less mobile at all but flood flows. Conversely, sediment mobility was nearly uniform in the plane bed channel across all flows.

3.3.4 | Redd dewatering

Viable spawning habitat, based on depth and velocity requirements, varied between the channel forms. Nearly 50% of the bankfull channel provided viable spawning habitat in the pool–riffle compared with only 31% in the plane bed. Pool–riffle spawning habitat was extensive and patchy, excluding only excessively high velocity zones on the riffle crests. Alternatively, plane bed spawning habitat only occurred in 1- to 2-m bands along the wetted channel margins with sufficiently low velocity to meet predefined spawning requirements.

Redd dewatering risk within viable spawning habitat areas also varied significantly across flow–form scenarios. Redd dewatering risk was greater in the plane bed than the pool–riffle at base flow (100% vs. 57% of spawning habitat) but risk was maintained across a greater range of flows (0.2–0.4× bankfull flow) in the pool–riffle. This is because the pool–riffle morphology has more gradual side slopes, and the total available spawning habitat is greater. High dewatering risk (>30% of spawning habitat) occurred only in the dry altered scenario, with very low flows occurring throughout the redd incubation (October–December) and emergence (January–March) periods.

4 | DISCUSSION

4.1 | The utility of synthetic river archetypes

This study demonstrated the ability to synthesize DTMs from channel classification archetypes exhibiting distinct ecosystem function performance, offering a scientifically transparent, repeatable, and adjustable framework for flow–form–function inquiry. Specific geomorphic attribute values were accurately represented by the synthetic morphologies, including channel dimensions, cross-sectional geometry, depth and width variability, sinuosity, and slope (Figure 3). The flow convergence routing mechanism was shown to occur in the pool–riffle archetype but not in the plane bed one, confirming that the two morphologies were capturing distinct geomorphic maintenance processes as distinguished by the Sacramento Basin channel classification (Lane, Pasternack, et al., 2017). Once a person understands how to produce a synthetic DTM with the required subreach-scale variability to drive geomorphic processes and ecological functions, then the software implements that very quickly. As a result, time and financial requirements are dramatically reduced compared with doing a field-based campaign involving meter-resolution topographic surveying, parameter calibration, and quality assurance procedures. This approach therefore liberates future research to explore and isolate a larger range of flow and form characteristics than those considered in the present study. This is an important first step for evaluating how different kinds of rivers function, but care should be used in extrapolating the specific results to any specific actual channel topography for real river management. Archetypal studies provide useful guidelines and then local studies should be conducted to ascertain how the mechanisms play out in their details in the local setting, possibly including validation efforts, to the extent feasible.

To choose the correct permutation of depth and width parameters to the synthetic morphologies, expert judgment was used based on field experience and understanding of how to interpret the processes associated with different patterns of topographic variability. However,

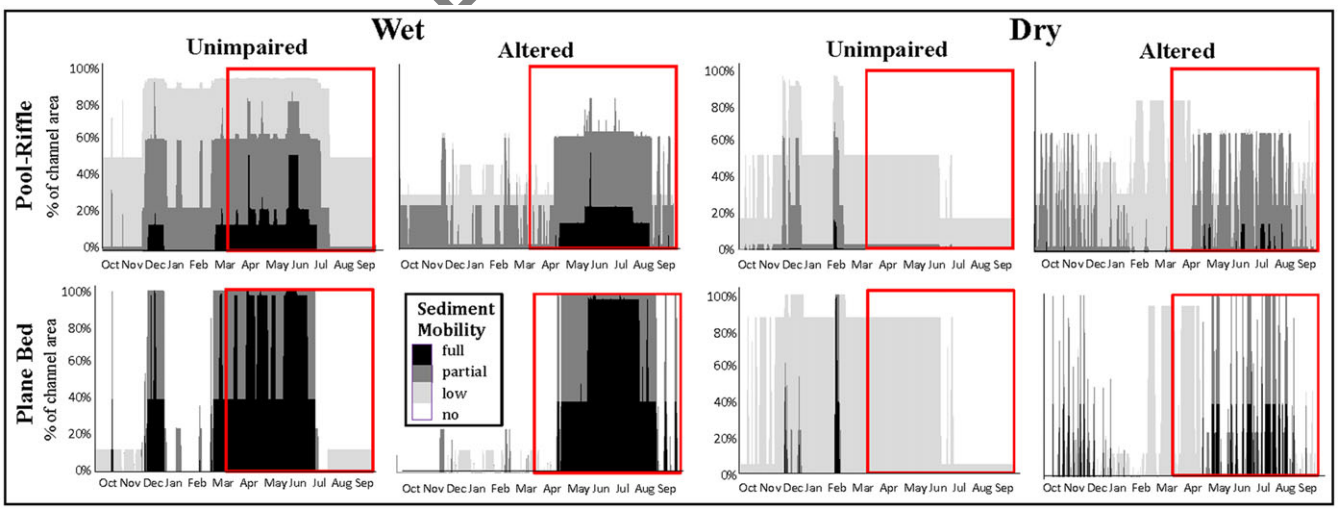

FIGURE 8 Daily time series plots of the proportion of the bankfull channel exhibiting different tiers of sediment mobility illustrate the performance of salmonid bed preparation (boxed, partial/high mobility from April–September) and occupation (no/low mobility from October–March) functions

some attributes required to generate representative topographic attributes, such as floodplain width variability and floodplain lateral slope, were not available in the channel classification of Lane, Pasternack, et al. (2017). This represents an important limitation of the proposed method, because useful results for certain ecosystem functions (e.g., riparian recruitment) require better information than is currently available. More datasets focusing on different aspects of geomorphic variability at different scales would enable more informed metric and parameter choices (Brown & Pasternack, 2017).

4.2 | Ecological significance of specific patterns of topographic variability

The spatial and temporal distributions of depth and velocity across channel forms illustrate differences in sensitivity to flow changes, with major implications for ecosystem functioning and aquatic biodiversity (Dyer & Thoms, 2006). The pool–riffle morphology was less sensitive to temporal changes in flow in terms of associated changes in depth and velocity, but more spatially variable, exhibiting a larger range and CV of depth and velocity values for a given discharge. This indicates that the pool–riffle has more sustained persistence of hydraulic patterns, making many ecosystem functions less prone to temporal fluctuations with flow as long as the discharges fall below the threshold for particular processes (Gostner, Parasiewicz, et al., 2013).

Study results support emerging scientific understanding that many river ecosystem functions are controlled by subreach-scale topographic variability (Brown & Pasternack, 2016; Murray, Thoms, & Rayburg, 2006; Thompson, 1986; White et al., 2010) by quantifying the occurrence of distinct ecosystem functions in reaches of high versus low topographic variability. Specifically, results emphasize that it is not enough to just obtain random topographic variability or any arbitrary coherent permutation of variability but rather the pattern of organized variability must meet the requirements of the appropriate GCS and dominant geomorphic processes for that channel archetype (Brown et al., 2015; Brown & Pasternack, 2014).

Distinct spatial and temporal hydraulic patterns identified in this study but not explicitly incorporated into performance metrics highlight important future directions for this methodology. For example, changes in spatial patterns of sediment mobility exhibited across flow–form combinations likely influence biological suitability for bed occupation in addition to the magnitude- and timing-based performance metrics considered here. The temporal patterns of bed mobility also varied substantially within the bed occupation and preparation periods (Figure 7), which was not captured by the selected performance metrics. More information about the spatio-temporal hydraulic requirements for particular species and life stages and improved metrics for quantifying these characteristics would refine performance estimates within the proposed framework.

4.3 | Flow and form controls on ecosystem functioning

Five Mediterranean-montane river ecosystem functions related to geomorphic variability and aquatic habitat were evaluated in the context of interacting flow (i.e., water year type and hydrologic impairment) and form (i.e., morphology type) controls on ecohydraulic response (Figures 5 and 6). Flow convergence routing was controlled primarily by channel form, as it only occurred in the pool–riffle morphology. However, sufficiently high flows were also needed for a shear stress reversal to occur in support of the mechanism. Hydrogeomorphic diversity was controlled primarily by channel form, and specifically topographic variability, as expected. More surprisingly, HMID was also influenced by flow attributes, with water year type, hydrologic impairment, and morphology type all playing significant and interacting roles in the ecohydraulic response. Salmonid bed preparation and occupation illustrate trade-offs in all three controlling variables, with bed preparation performing best in the wet, altered, plane bed scenario, whereas bed occupation performed best in the dry, unimpaired pool–riffle morphology. The duration and timing of redd dewatering risk were controlled by water year type and hydrologic impairment, whereas the magnitude of dewatering risk, based on the proportion of spawning habitat exhibiting sufficiently low depth or velocity, was controlled solely by channel form. These results emphasize the complex interacting flow and form controls on key ecosystem functions and the differences in dominant controls between ecosystem functions.

HMID performance trade-offs in particular provide insight for environmental water management, given the common conception that increased habitat heterogeneity promotes biodiversity (Dyer & Thoms, 2006). The highest HMID was exhibited by the pool–riffle under dry unimpaired conditions. However, under hydrologic impairment, HMID was higher under the wet pool–riffle than the dry plane bed scenario for all but the lowest flows. This finding indicates a trade-off between flow and form with respect to diversity whereby either increasing topographic variability (i.e., plane bed to pool–riffle) or increasing the number of low flow days in the flow regime (i.e., wet to dry water year type) was capable of increasing overall spatio-temporal diversity. In such instances, knowledge of flow–form interactions could be used to guide more nuanced, targeted management efforts to promote ecological end goals such as increased biodiversity.

In general, bed occupation performed poorly across all flow and form scenarios. This finding may be due to the coarse bankfull stage discretization used in the study (eight discharges from 0.2–2× bankfull stage, Table 1), allowing lower daily discharge values to be associated with higher sediment mobility than occurs in reality. Results such as these can inform future studies by promoting iterative modification of decisions such as the bankfull stage discretization and the range of discharges considered to improve representation of ecosystem functions within the proposed methodology.

4.4 | Implications for environmental management

The quantitative metrics of relative performance across a suite of ecosystem functions highlighted critical performance trade-offs, emphasizing the significance of spatio-temporal diversity of flow and form at multiple scales for maintaining river ecosystem integrity. For example, the pool–riffle morphology supported flow convergence routing and promoted high hydraulic diversity and salmonid bed occupation, whereas the plane bed morphology supported salmonid bed preparation and provided habitats of reduced dewatering stress for salmonid

redds during dry years. These results indicate that restoring or designing a pool–riffle dominated stream network to provide interspersed plane bed reaches may support higher overall ecosystem integrity by promoting distinct and complementary functions in different locations during biologically significant periods. Such findings support the emerging recognition of spatial and temporal heterogeneity as fundamental characteristics of fluvial systems and the need for a flexible framework within which natural processes, such as sediment transport and nutrient dynamics, can occur (Clarke, Bruce-Burgess, & Wharton, 2003; Gostner, Parasiewicz, et al., 2013; Vanzo et al., 2016; Escobar-Arias & Pasternack, 2010).

With respect to hydrologic variability, only wet years supported high performance of salmonid bed preparation and shear stress reversals, whereas dry years significantly increased hydraulic diversity and availability of fall-run Chinook spawning habitat. A range of wet to dry years is required to support the full suite of ecosystem functions considered here. Interannual variability plays a key role (in concert with spatial variability of form and bed substrate) in maintaining river ecosystem integrity. This finding also indicates the potential for changes or losses in function under a changing climate in which the spectrum or the ratio of wet to dry years is significantly altered from that to which native riverine species are adapted (Null & Viers, 2013). For example, fewer sufficiently wet years to generate shear stress reversals in pool–riffle reaches may compromise their ability to maintain high topographic variability, thus shifting the suite of ecosystem functions supported in these reaches towards those already supported by plane bed reaches. This would reduce ecological variability and thus overall ecological resilience of the stream network.

This application of synthetic datasets to flow–form–function inquiry provides a foundation for transitioning from expressing ecosystem impacts and responses in terms of fixed flow or form features to spatio-temporally varying hydrogeomorphic dynamics along a spectrum of alterations of the synthetic datasets. The simple, process-based framework proposed here is expected to elucidate key processes and thresholds underlying spatial and temporal dynamics of river ecosystems through future applications. For instance, the functional role and alteration thresholds of individual geomorphic attributes (e.g., confinement and channel bed undulations) could be isolated through iterative generation and evaluation of numerous synthetic channel forms. This information is expected to improve understanding of ecosystem resilience and the potential for rehabilitation projects under current and future hydrogeomorphic alterations.

4.5 | Study uncertainty

Uncertainties in the ecosystem functions model developed here include uncertainty in model completeness, parameters, and data inputs. With respect to model completeness, this study explicitly incorporated attributes of key hydrologic and geomorphic processes controlling river ecosystem functions for more complete evaluation of controlling variables and their dynamic interactions. However, several critical aspects of river ecosystems including water quality, temperature, population dynamics, and morphodynamics are not considered in the scope of the current study.

Model parameter uncertainties are derive from parameter and equation selection. For example, the depth slope product shear stress equation assumes steady uniform flow, which is appropriate for the geomorphic archetypes considered here under steady discharges but should be assessed on a case-by-case basis for application to real channel morphologies (Brown & Pasternack, 2008; Pasternack et al., 2008). The use of Shields parameter thresholds to delimit sediment transport stages provided a simple approach to explore flow–hydrogeomorphic process relationships, but there is uncertainty associated with these thresholds and others could be selected depending on the application or with more information regarding bed composition. The spatial and temporal thresholds of ERHPs constraining the ecosystem functions are also uncertain. For instance, the requirement of seven consecutive days of flooding for riparian recruitment is an estimate based on field studies across the Sierra Nevada that exhibit high variability between sites.

Data input uncertainties originate from the streamflow time series and river corridor morphologies. In the current application, stage–discharge relationships were the main source of hydrologic uncertainty, as they were manually estimated for the Yuba River in the absence of established rating curves. Rating curves derived from field measurements would substantially reduce this source of uncertainty. The use of real streamflow time series minimized uncertainty associate with hydrologic inputs. However, the use of modelled streamflow or hydrologic archetypes, as proposed for future applications, would create additional uncertainty. Uncertainties arising from the use of synthetic river valleys morphologies include field measurements of reach-averaged geomorphic attributes including the CV of width and depth. The frequency and distribution of width and depth measurements used in these calculations will influence variability estimates, and as a result, the synthesized topographies. More research is needed to evaluate the influence of different sampling schemes and measures of topographic variability on the synthesized DTMs and dependent hydrogeomorphic processes.

5 | CONCLUSIONS

This study tackles key questions regarding the utility of synthetic DTMs for ecohydraulic analysis, the ecological significance of topographic variability, how to evaluate the ecological impacts of different flow–form settings or types of river restoration efforts, and whether (re) instatement of key flow or form attributes is likely to restore ecological processes (National Research Council, 2007). The development and application of simple, quantitative ecosystem performance metrics enabled evaluation of the ecohydraulic response to changes in flow and/or form settings typical of Mediterranean-montane rivers. By comparing these performance metrics across individual and combined adjustments to flow and form attributes, this study provides a novel framework for assessing and comparing ecosystem function performance under natural and human altered flow regimes and river corridor morphologies. Moreover, this research demonstrates the significance of spatio-temporal diversity of flow (seasonal and interannual) and form (channel shape and bed substrate) and their interactions for supporting distinct ecosystem functions that maintain river ecosystem integrity.

ACKNOWLEDGEMENTS

This research was supported by the UC Davis Hydrologic Sciences Graduate Group Fellowship and the USDA National Institute of Food and Agriculture, Hatch project numbers #CA-D-LAW-7034-H and CA-D-LAW-2243-H. The authors also acknowledge Rocko Brown for instrumental discussions of synthetic river corridors and Helen Dahlke for valuable discussions about hydrology and geomorphology.

ORCID

Belize A. Lane http://orcid.org/0000-0003-2331-7038
Gregory B. Pasternack http://orcid.org/0000-0002-1977-4175

REFERENCES

Abu-Aly, T. R., Pasternack, G. B., Wyrick, J. R., Barker, R., Massa, D., & Johnson, T. (2014). Effects of LiDAR-derived, spatially distributed vegetation roughness on two-dimensional hydraulics in a gravel-cobble river at flows of 0.2 to 20 times bankfull. *Geomorphology*, *206*, 468–482.

Brown, R. A., & Pasternack, G. B. (2008). Engineered channel controls limiting spawning habitat rehabilitation success on regulated gravel-bed rivers. *Geomorphology*, *97*, 631–654.

Brown, R. A., & Pasternack, G. B. (2014). Hydrologic and topographic variability modulate channel change in mountain rivers. *Journal of Hydrology*, *510*, 551–564.

Brown, R. A., & Pasternack, G. B. (2016). Analyzing bed and width oscillations in a self-maintained gravel-cobble bedded river using geomorphic covariance structures. *Earth Surface Dynamics Discussions*, *4*, 1–48.

Brown, R. A., & Pasternack, G. B. (2017). Bed and width oscillations form coherent patterns in a partially confined, regulated gravel–cobble-bedded river adjusting to anthropogenic disturbances. *Earth Surface Dynamics*, *5*, 1–20.

Brown, R. A., Pasternack, G. B., & Lin, T. (2015). The topographic design of river channels for form-process linkages. *Environmental Management*, *57*, 929–942.

Brown, R. A., Pasternack, G. B., & Wallender, W. W. (2014). Synthetic river valleys: Creating prescribed topography for form–process inquiry and river rehabilitation design. *Geomorphology*, *214*, 40–55.

Buffington, J. M., & Montgomery, D. R. (1997). A systematic analysis of eight decades of incipient motion studies, with special reference to gravel-bedded rivers. *Water Resources Research*, *33*, 1993–2029.

Caamaño, D., Goodwin, P., Buffington, J. M., Liou, J. C., & Daley-Laursen, S. (2009). Unifying criterion for the velocity reversal hypothesis in gravel-bed rivers. *Journal of Hydraulic Engineering*, *135*, 66–70.

Clarke, S. J., Bruce-Burgess, L., & Wharton, G. (2003). Linking form and function: Towards an eco-hydromorphic approach to sustainable river restoration. *Aquatic Conservation: Marine and Freshwater Ecosystems*, *13*, 439–450.

Cullum, C., Brierley, G., Perry, G. L. W., & Witkowski, E. T. F. (2017). Landscape archetypes for ecological classification and mapping. *Progress in Physical Geography*, *41*, 95–123.

Doyle, M. W., Stanley, E. H., Strayer, D. L., Jacobson, R. B., & Schmidt, J. C. (2005). Effective discharge analysis of ecological processes in streams. *Water Resources Research*, *41*, W11411.

Dyer, F. J., & Thoms, M. C. (2006). Managing river flows for hydraulic diversity: An example of an upland regulated gravel-bed river. *River Research and Applications*, *22*, 257–267.

Escobar-Arias, M. I., & Pasternack, G. B. (2010). A hydrogeomorphic dynamics approach to assess in-stream ecological functionality using the functional flows model, part 1-model characteristics. *River Research and Applications*, *26*, 1103–1128.

Escobar-Arias, M. I., & Pasternack, G. B. (2011). Differences in river ecological functions due to rapid channel alteration processes in two California rivers using the functional flows model, part 2-model applications. *River Research and Applications*, *27*, 1–22.

Gasith, A., & Resh, B. (1999). Streams in Mediterranean regions: Abiotic influences and biotic responses to predictable seasonal event. *Annual Review of Ecological Systems*, *30*, 51–81.

Gostner, W., Alp, M., Schleiss, A. J., & Robinson, C. T. (2013). The hydro-morphological index of diversity: a tool for describing habitat heterogeneity in river engineering projects. *Hydrobiologia*, *712*, 43–60.

Gostner, W., Parasiewicz, P., & Schleiss, A. J. (2013). A case study on spatial and temporal hydraulic variability in an alpine gravel-bed stream based on the hydromorphological index of diversity. *Ecohydrology*, *6*, 652–667.

Hanak, E., Lund, J., Dinar, A., Gray, B., Howitt, R., Mount, J., … Thompson, B. (2011). *Managing California's water: From conflict to reconciliation*. San Francisco, CA: Public Policy Institute of California.

Healey, M. C. (1991). Life history of chinook salmon (*Oncorhynchus tshawytscha*). In C. Groot, & L. Margolis (Eds.), *Pacific salmon life histories*. Vancouver, British Columbia: University of British Columbia Press.

Jackson, J. R., Pasternack, G. B., & Wheaton, J. M. (2015). Virtual manipulation of topography to test potential pool–riffle maintenance mechanisms. *Geomorphology*, *228*, 617–627.

Jacobson, R. B., & Galat, D. L. (2006). Flow and form in rehabilitation of large-river ecosystems: An example from the Lower Missouri River. *Geomorphology*, *77*, 249–269.

Jowett, I. G. (1993). A method for objectively identifying pool, run, and riffle habitats from physical measurements. *New Zealand Journal of Marine and Freshwater Research*, *27*, 241–248.

Kasprak, A., Hough-Snee, N., Beechie, T., Bouwes, N., Brierley, G., Camp, R., … Wheaton, J. (2016). The blurred line between form and process: A comparison of stream channel classification frameworks. *PLoS One*, *11*, e0150293.

Konrad, C. P., Booth, D. B., Burges, S. J., & Montgomery, D. R. (2002). Partial entrainment of gravel bars during floods. *Water Resources Research*, *38*, 9-1–9-16.

Lai, Y. G. (2008). *SRH-2D version 2: Theory and user's manual*. Denver, CO: U.S. Department of the Interior.

Lane, B. A., Dahlke, H. E., Pasternack, G. B., & Sandoval-Solis, S. (2017). Revealing the diversity of natural hydrologic regimes in California with relevance for environmental flows applications. *Journal of American Water Resources Association (JAWRA)*, *53*(2), 411–430.

Lane, B. A., Pasternack, G. B., Dahlke, H. E., & Sandoval-Solis, S. (2017). The role of topographic variability in river channel classification. *Physical Progress in Geography*, *41*(5), 570–600.

MacWilliams, M. L., Wheaton, J. M., Pasternack, G. B., Street, R. L., & Kitanidis, P. K. (2006). Flow convergence routing hypothesis for pool-riffle maintenance in alluvial rivers. *Water Resources Research*, *42*, W10427.

Magilligan, F. J., & Nislow, K. H. (2005). Changes in hydrologic regime by dams. *Geomorphology*, *71*, 61–78.

Montgomery, D. R., & Buffington, J. M. (1997). Channel-reach morphology in mountain drainage basins. *GSA Bulletin*, *109*(5), 596–611.

Moyle, P. B., & Randall, P. J. (1998). Evaluating the biotic integrity of watersheds in the Sierra Nevada, California. *Conservation Biology*, *12*, 1318–1326.

Murray, O., Thoms, M., & Rayburg, S. (2006). The diversity of inundated areas in semiarid flood plain ecosystems. In *Sediment dynamics and the hydromorphology of fluvial systems*. Dundee, UK: IAHS Publication.

National Research Council (2007). *River science at the U.S. Geological Survey*. In, edited by Committee on River Science at the U.S. Geological Survey, 206. Washington, D.C.: The National Academies Press.

Null, S. E., & Viers, J. H. (2013). In bad waters: Water year classification in nonstationary climates. *Water Resources Research*, *49*, 1137–1148.

Parasiewicz, P. (2007). Using MesoHABSIM to develop reference habitat template and ecological management scenarios. *River Research and Applications*, *23*, 924–932.

Pasternack, G. B. (2011). 2D modeling and ecohydraulic analysis (University of California at Davis).

Pasternack, G. B., Bounrisavong, M. K., & Parikh, K. K. (2008). Backwater control on riffle–pool hydraulics, fish habitat quality, and sediment transport regime in gravel-bed rivers. *Journal of Hydrology*, *357*, 125–139.

Poff, N. L., Allan, J. D., Bain, M. B., Karr, J. R., Prestegaard, K. L., Richter, B. D., … Stromberg, J. C. (1997). The natural flow regime: A paradigm for river conservation and restoration. *BioScience*, *47*, 769–784.

Poff, N. L. R., & Ward, J. V. (1990). Physical habitat template of lotic systems: Recovery in the context of historical pattern of spatiotemporal heterogeneity. *Environmental Management*, *14*, 629–645.

Price, A. E., Humphries, P., Gawne, B., Thoms, M. C., & Richardson, J. (2013). Effects of discharge regulation on slackwater characteristics at multiple scales in a lowland river. *Canadian Journal of Fisheries and Aquatic Sciences*, *70*, 253–262.

Richards, K. S. (1976). The morphology of riffle-pool sequences. *Earth Surface Processes*, *1*, 71–88.

Richter, B. D., & Richter, H. E. (2000). Prescribing flood regimes to sustain riparian ecosystems along meandering rivers. *Conservation Biology*, *14*(5), 1467–1478.

Sandoval-Solis, S., McKinney, D. C., & Loucks, D. P. (2010). Sustainability index for water resources planning and management. *Journal of Water Resources Planning and Management*, *137*, 381–390.

Scown, M. W., Thoms, M. C., & De Jager, N. R. (2015). An index of floodplain surface complexity. *Hydrology and Earth System Sciences Discussions*, *12*, 4507–4540.

Small, M. J., Doyle, M. W., Fuller, R. L., & Manners, R. B. (2008). Hydrologic versus geomorphic limitation on CPOM storage in stream ecosystems. *Freshwater Biology*, *53*, 1618–1631.

Soulsby, C., Youngson, A. F., Moir, H. J., & Malcolm, I. A. (2001). Fine sediment influence on salmonid spawning habitat in a lowland agricultural stream: A preliminary assessment. *Science of the Total Environment*, *265*, 295–307.

Thompson, A. (1986). Secondary flows and the pool-riffle unit: A case study of the processes of meander development. *Earth Surface Processes and Landforms*, *11*, 631–641.

U.S. Fish and Wildlife Service (2010a). *Flow-habitat relationships for spring and fall-run Chinook salmon and steelhead/rainbow trout spawning in the Yuba River*. In, 127. Sacramento, CA: The Energy Planning and Instream Flow Branch.

U.S. Fish and Wildlife Service (2010b). *Yuba River redd dewatering and juvenile stranding report*. In, 60. Sacramento, CA: Energy Planning and Instream Flow Branch, .

Vanzo, D., Zolezzi, G., & Siviglia, A. (2016). Eco-hydraulic modelling of the interactions between hydropeaking and river morphology. *Ecohydrology*, *9*, 421–437.

White, J. Q., Pasternack, G. B., & Moir, H. J. (2010). Valley width variation influences riffle–pool location and persistence on a rapidly incising gravel-bed river. *Geomorphology*, *121*, 206–221.

Wohl, E., Bledsoe, B. P., Jacobson, R. B., Leroy Poff, N., Rathburn, S. L., Walters, D. M., & Wilcox, A. C. (2015). The natural sediment regime in rivers: Broadening the foundation for ecosystem management. *BioScience*, *65*, 358–371.

Wohl, E., & Merritt, D. (2005). Prediction of mountain stream morphology. *Water Resources Research*, *41*, W08419.

Wolman, M. G., & Miller, J. P. (1960). Magnitude and frequency of forces in geomorphic processes. *The Journal of Geology*, *68*(1), 54–74.

Worthington, T. A., Brewer, S. K., Farless, N., Grabowski, T. B., & Gregory, M. S. (2014). Interacting effects of discharge and channel morphology on transport of semibuoyant fish eggs in large, altered river systems. *PLoS One*, *9*, e96599.

Yarnell, S. M., Lind, A. J., & Mount, J. F. (2012). Dynamic flow modelling of riverine amphibian habitat with application to regulated flow management. *River Research and Applications*, *28*, 177–191.

Yoshiyama, R. M., Fisher, F. W., & Moyle, P. B. (1998). Historical abundance and decline of Chinook salmon in the Central Valley Region of California. *North American Journal of Fisheries Management*, *18*, 487–521.

SUPPORTING INFORMATION

Additional Supporting Information may be found online in the supporting information tab for this article.

How to cite this article: Lane BA, Pasternack GB, Sandoval-Solis S. Integrated analysis of flow, form, and function for river management and design testing. *Ecohydrology*. 2018;e1969. https://doi.org/10.1002/eco.1969